Title

Exploring the elasticity and adhesion behavior of cardiac fibroblasts by atomic force microscopy indentation

Authors

Codan, B
Del Favero, G
Martinelli, V
et al.

Publication Date

2014-07-01

DOI

10.1016/j.msec.2014.04.003

Peer reviewed

Published in final edited form as:
Mater Sci Eng C Mater Biol Appl. 2014 July 1; 40: 427–434. doi:10.1016/j.msec.2014.04.003.

Exploring the elasticity and adhesion behavior of cardiac fibroblasts by atomic force microscopy indentation

B. Codan[1], **G. Del Favero**[1], **V. Martinelli**[1,2], **C.S. Long**[3], **L. Mestroni**[3], and **O. Sbaizero**[1]

[1]Department of Engineering and Architecture University of Trieste – Italy

[2]International Center for Genetic Engineering and Biotechnology Trieste - Italy

[3]University of Colorado Cardiovascular Institute University of Colorado Denver - Aurora, CO-U.S.A

Abstract

AFM was used to collect the whole force-deformation cell curves. They provide both the elasticity and adhesion behavior of mouse primary cardiac fibroblasts. To confirm the hypothesis that a link exists between the membrane receptors and the cytoskeletal filaments causing therefore changing in both elasticity and adhesion behavior, actin-destabilizing Cytochalsin D was administrated to the fibroblasts. From immunofluorescence observation and AFM loading/unloading curves, cytoskeletal reorganization as well as a change in the elasticity and adhesion was indeed observed.

Elasticity of control fibroblasts is three times higher than that for fibroblasts treated with 0.5 μM Cytochalasin. Moreover, AFM loading-unloading curves clearly show the different mechanical behavior of the two different cells analyzed: (i) for control cells the AFM cantilever rises during the dwell time while cells with Cytochalasin, fail to show such an active resistance. (ii) the maximum force to deform control cells is quite higher and as far as adhesion is concern (iii) the maximum separation force, detachment area and the detachment process time are much larger for control compared to the Cytochalasin treated cells. Therefore, alterations in the cytoskeleton suggest that a link must exist between the membrane receptors and the cytoskeletal filaments beneath the cellular surface and inhibition of actin polymerization has effects on the whole cell mechanical behavior as well as adhesion.

Keywords

Cell; Adhesion; Cardiac fibroblast; AFM

Corresponding author: Orfeo Sbaizero, Phone +39 040 558 3770 Fax: +39 040 57 20 44, sbaizero@units.it.

1. INTRODUCTION

Like bubbles, a membrane that separates the contents from the outside environment characterizes cells. However, there are major dissimilarities: the cell interior contains the cytoskeleton, a gel composed of cross-linked, long-chain proteins; this provides the cell with shear rigidity and shape integrity. The cytoskeleton contains several structures: actin, microtubules and intermediate filaments, each of which has different elastic properties [1]. Furthermore, the cell shape is regulated by several factors among them (i) the cell proliferation and metabolism, (ii) the internal forces generated by the cytoskeleton, (iii) cell motility, and (iv) the properties of the extra-cellular matrix (ECM). For instance, there are examples of curved membrane proteins responsible for inducing concave or convex curvature [2]. Moreover, these membrane proteins are known to promote actin polymerization that can induce the spontaneous initiation of membrane protrusions [3–4]. The cell membrane curvature is therefore crucial since it finalizes the connection between the membrane shape and membrane proteins density, allowing an increase in cytoskeletal forces acting on the membrane and eventually promoting new cell protrusions. It is has also been shown that the membrane adhesion molecules such as integrins, aggregate at regions of high convex membrane curvature [5–9]. Cell adhesion to extracellular matrix (ECM) is mediated by integrins, proteins that regulate and couple the ECM to the actin cytoskeleton filaments [10]. These adhesion membrane proteins are therefore accountable for the recruitment of actin polymerization to the membrane and to the membrane tension due to the adhesion with the extracellular matrix or from the force of actin polymerization, and both forces regulate the cell shape. Furthermore, the ECM-integrin-actin “bridge” provides an important physical connection between the ECM and cytoskeleton for bi-directionally transducing external forces into biochemical signals and forces from the cytoskeleton to the extracellular environment [11–12].

Alterations in the cell adhesive properties trigger numerous pathologies and disease processes such as in metastasic diffusion [13–16], and muscular dystrophies [17– 18].

Atomic force microscopy (AFM) is particularly useful in studying interactions between biological molecules since it allows molecular resolution imaging in aqueous media [19–20]. In particular it is well suited for studying the evolution of adhesion forces between the AFM tip (normally a microsphere) and the cell membrane. Typically in this test, the cells are plated on the substrate and in contact with the cantilever only during force measurement. The AFM indenter is moved toward the cell membrane, comes into contact with it, the microsphere is allowed to adhere on the cell membrane during the holding period. Upon retraction, the AFM sphere adheres to the cell membrane and causes opposite deflections of the probe compared to the loading process, therefore the adhesion force can be assessed during the unloading cycle. Such events are typically related to protein unfolding [21] and receptor–ligand binding [22]. Considerations about adhesion and detachment forces such as force steps and tether extraction forces might also be evaluated from unloading curves. Furthermore, the area between the loading and unloading curves reflect viscoelastic cell hysteresis. Based on these considerations, it is our belief that the study of whole-cell AFM force-deformation curves, during a loading and unloading cycle, provides more comprehensive insight into cell biomechanical behavior.

In particular, this study focuses on the cardiac fibroblast, the cell responsible for the structural integrity of the heart but also responsible for the pathologic myocardial fibrosis commonly found in association with cardiac hypertrophy, cardiomyopathy and failure. Fibrosis results in cell morphology changes, cytoskeletal alterations, and overall in changes in the bulk mechanical properties of the myocardial tissue [23, 24]. In cardiomyopathy cytoskeletal proteins mutations could trigger this pathology, involving alterations of the membrane-associated proteins [25, 26].

In this paper, elasticity, viscoelasticity and adhesion behavior of mouse primary cardiac fibroblasts by AFM indentation has been measured. The main focus of this study was to investigate cell elasticity, cell adhesion and it relationship with cytoskeletal organization. The capability of AFM to simultaneously measure cellular mechanical properties and adhesion forces make it an ideal technique to test the hypothesis that adhesion behavior is related to the integrin density, cytoskeletal alterations, and changes in the cell elasticity and therefore that membrane receptors that are physically connected with cytoskeletal elements serve as a link between the external mechanical environment and the internal signaling of the cell. To understand to what extent the adhesion as well as elastic properties are linked and triggered by parts of the cytoskeleton, we used Cytochalasin D to alter the polymerization kinetics of the actin cytoskeleton filaments.

AFM force-deformation curves method is already used to measure cell elasticity and the use of drugs like Cytochalsin to chemically disassemble the actin network is also well known; for instance, Rotsch et al. [27] found that cultured rat liver macrophages treated with this drug have an average elastic modulus seven-fold less than control cells. However, this paper emphasizes that the whole force-deformation curve carries several information (1) the total force required to deformed the nucleus (2) the AFM cantilever deformation at the holding point, (3) the hysteresis area between the loading and unloading cycle, and (4) the area under the deformation curves during the unloading cycle which reflects the cell adhesion behavior. Even if every piece of information is well known in general, it is normally used as a single evidence. In our case we correlate all information to the mechanical properties as well as adhesion behavior of very interesting cells like cardiac fibroblasts.

2. MATERIALS AND METHODS

2.1. Culture of Adult Cardiac Fibroblasts

Primary expanded culture of cardiac fibroblast was established from adult C57 mice in agreement to institutional guidelines and in compliance with national and international laws and policies (European Economic Community Council Directive 86/609, OJL 358, December 12, 1987). Briefly, whole hearts were extracted, rinsed with CBFHH (Calcium and Bicarbonate Free Hanks with Hepes, composition in mM: NaCl 137; KCl 5.36; Mg_2SO_4 0.81; Dextrose 5.55; KH_2PO_4 0.44; Na_2HPO_4 $7H_2O$ 0.34; Hepes 20.04; pH=7.4) and minced into pieces. Tissue was rinsed twice with digesting solution (Trypsin 1.75mg/mL and DNAase 10 μg/mL in CBFHH) and supernatant was discarded. Every cycle of tryptic digestion was performed placing tissue suspension on a stir plate for 10 minutes and gently pipetting up and down the tissue 10 times. To ensure maximal collection of fibroblasts at least 8–10 digestion cycles were performed. At the end of the digestion cells were

centrifuged (1500 rpm, 10 minutes, RT). Cells re-suspended in complete medium (DMEM Glutamax high glucose 4.5 g/l and 20 % Fetal Bovine Serum, Gibco) and kept in culture at sub-confluent density and seeded according to experimental need.

2.2.Immunofluorescence

Cells grown on p35 plates (Falcon, Becton Dickinson, USA) were fixed in PBS containing 3.5% PFA for 20 min; aldehydes were quenched with 0.1 M glycine in PBS for 10 min at room temperature. Cell were permeabilized with 1% Triton X-100 for 30 min, blocked with 2% BSA and 0.05% sodium azide in PBS (blocking buffer) for 1 h at room temperature. F-Actin filaments were labeled with FITC fluorescent conjugated Phalloidin for 1 h at room temperature. (1:20, P5282, SIGMA). Cells were then washed three times for 10 min with PBS and 0.05% Tween 20. Samples were mounted in Vectashield plus DAPI to stain the nuclei (Vector Laboratories).

2.3 AFM measurements

An AFM Solver Pro-M (NT-MDT, Moscow, Russia) was used to acquire morphology as well as force-displacement curves. The AFM was equipped with a “liquid cell” setup with a standard cantilever holder cell for operating in liquid at controlled temperature. Commercially available cantilevers having tips of polystyrene microsphere (Diameter about 10 μm by scanning electron microscopy imaging) coated with a gold layer were used (PNP-DB, Nanoworld, Neuchatel, Switzerland). The cantilevers force constant was calibrated using the thermal fluctuations method. For soft biological samples it is suggested to use spherical probes since the force is applied to a broader cell area than would be the case if a sharp tip is used, resulting in a lower pressure and less cell damage. But this is not the only reason to prefer spherical indenters. Cells or tissues are very inhomogeneous, consisting of different components (nucleus, cytoskeletal components, etc.), therefore a sphere tip will return better data for such inhomogeneous materials. AFM probes were cleaned, prior to the indentation experiments, by submerging them successively in ethanol and chloroform (30 min each), in order to remove contaminant molecules adsorbed on the probe surface. All studies were performed on living, intact cells in cell culture medium. Only well-spread and isolated cells were investigated. Those with a round shape and a dark edge were rejected. The basic AFM technique for quantitative analysis of the cell elasticity is the force spectroscopy (called force-curve analysis). The relation between displacement and indentation of the cantilever in contact with the cell was obtained on advancing and retracting curves, called force curves representing the loading and unloading force. Force curves were collected by monitoring cantilever deflection while moving the piezoscanner resulting in a plot of force versus sample position (see Fig. 1). Indentation depth is calculated comparing the curve detected on the glass substrate and the curve recorded on the cell. To calibrate the cantilever deflection signal, curves of force versus the piezo displacement were acquired on the hard substrate of the cells (glass). The AFM tip was moved toward the cell with speeds of 0.5 μm/s. The speed range was chosen to avoid cell movement (at low compression speed) or hydrodynamic force contribution (significant at high speed). To minimize the possible damage to the cell membrane and contamination of the AFM tip, the cells were not scanned before the indentation experiments. Measurements performed around the nucleus are less affected by artifact due to the substrate stiffness [28].

The distal regions, away from the nucleus, were therefore avoided. For each experimental condition, at least 18 cells data are collected, 4 force curves are acquired for every cell, making a grid around the nucleus. In the case of cells treated with Cytochalasin D only 2 force curves are acquired for every cell, however more cells have been tested to acquire the same curve number. These data were enough to detect statistically significant differences. The test duration was never longer than 40 min to ensure cell viability. Different tests with AFM on contact and tapping mode had been performed to assess the impact of the acquisition mode on cells. No differences were recorded in terms of membrane alteration, while higher spatial resolution is guaranteed by contact mode. Force-deformation curve for single cell compression were plotted as loading force versus relative cell deformation. To quantify the cell compression, relative deformation, ε (cell height change/initial cell height), is used since the cell height varies.

2.4. Cell-AFM tip adhesion

Adhesion can be studied at two levels: single molecule and multiple events. Our tests were specially designed to operate in the latter mode where large number of adhesion events are involved. Upon retraction (unloading curve), the AFM sphere may adhere to the cell membrane and cause opposite deflections of the probe compared to the loading process. Such events are typically related to protein unfolding [29] and receptor–ligand binding [30]. Due to the stochastic nature of these events, several measurements need to be averaged to obtain reliable results. Interaction forces involved in these measurements range from tens to hundreds of picoNewtons. The noise level of a force curve due to AFM system and turbulence of the liquid is of the order of tens of pN, thus, interaction events involving forces below this level are barely detectable and got usually undetected. In our tests, after loading the cell, the sphere tip was allow to hold for 4 min. to develop a good adhesion at the membrane/tip interphase. The AFM also permits different holding time on the surface between the loading and retraction portions of the force curves. Longer holding times (up to 15 min.) were examined but no change in the adhesion-de-adhesion phenomenon was seen. Due to the large area of interaction and to the contact time, multiple bonds might be formed leading to multiple rupture events. Unloading curves usually present a peak of force followed by a cascade of rupture events until complete detachment is achieved. The maximum peak of force in the retracting curve determines the detachment force. The evaluation of the unbinding forces from these loading-unloading curves is nontrivial since the measured rupture forces are small and are the result of multiple unbinding, sequential breaking, and possibly nonspecific molecular interactions, molecular stretching, etc. The work of adhesion (or de-adhesion) is therefore evaluated by integrating the area between the contact point on the surface and the last force interaction, which resulted in the cantilever returning to its null position.

The main limitation of commercial AFM systems when measuring adhesion is the low travel of the vertical piezo-elements. The vertical range for our systems was 15 μm.

2.5. Cell viscoelasticity

The force-curve analysis contains information about long- and short-range interactions and represents a basis for assessing the cell Young’s modulus. Furthermore, differences between

the loading and unloading curves reflect viscoelastic cell hysteresis. To quantify the relative amount of energy that was lost due to hysteresis during the AFM cell loading and unloading cycle, we compared the energy that was required to indent the cells and the energy that was recovered during the retraction. Any loss of energy will be visible as a difference between the curves. To quantify for each experiment the difference between the indentation and retraction energy, we calculated the integrals for all indentation and retraction curves.

2.6. Modeling cells elasticity

The Young's modulus (elasticity) is often used to describe mechanical properties of cells. Since the earliest AFM studies of soft biological samples, [31–32] the prevalent method of evaluating AFM indentation data to assess the elasticity (or Young Modulus) has been the so-called "Hertz-Sneddon model" of contact between two elastic bodies. The Hertz model assumes homogeneity, absolute cell elastic behavior and no interactions between sample and probe. But most biological materials are neither homogeneous nor absolutely elastic. The energy supplied by the indenter is not completely given back by a cell (as it would be done by an elastic material) but dissipates owing to plastic behavior that also appears as hysteresis between the loading and unloading force curves. The Hertz model is only valid for small indentations (up to 10% of the height of the cell) where the substrate doesn't influence the calculations. The original Hertz theory did not allow for adhesion of the indenter to the material; however, Johnson et al. modified the theory for this possibility [33]. The Hertz model gives an estimation of the cell elasticity and it is clear that in any case it will be afflicted by an error since it requires the assumption that contact surfaces are uninterrupted and frictionless and their deformations are insignificant. Although, in the case of cells, these assumptions do not correspond completely to reality due to the heterogeneous cell structure, the Hertz model is still useful for achieving information about cell elasticity. However, it be should pointed out that elasticity values calculated using various models differ from each other [34–35]. However, we believe that since all our tests have been performed following strictly the same protocol, results can give a good estimate of the cells elasticity. In the present paper, we used the Hertz-Sneddon model for sphere tips [36]:

$$F=\frac{4E\sqrt{R}}{3(1-\upsilon^2)}\delta^{3/2} \quad (1)$$

Where F is the load force, E is the Young modulus, ν the Poisson ratio, R is the sphere radius and "d" is the probe penetration into the cell. The Poisson's ratio was assumed to be 0.5 because the cell was considered incompressible.

2.7. Forces transfer through the cytoskeleton

To ascertain one potential force source transfer in both ways: from the nucleus through the cytoskeleton to the cell membrane and *vice versa*, in particular through actin filaments, we used the actin-destabilizing agent Cytochalasin D. In general, Cytochalasins have the ability to bind and block polymerization and the elongation of actin filaments. As a result of the inhibition of actin polymerization, Cytochalasins can cause an aggregation of filamentous actin into dispersed felt-like masses, therefore changing cellular morphology, and even causing cells to undergo apoptosis. The cardiac fibroblasts were treated with Cytochalasin D

at different concentrations between 0.5 and 4 μM. The drug was added to the cell culture dish 45 min. before experimentation, the first 30 min the cell culture was kept in the incubator, the last 15 min. under the AFM to stabilize the environment.

2.8. Statistics

Elasticity data were analyzed using R, data and are represented as box plots. The Kruskal-Wallis nonparametric test and the Dunn's posttest were used to compare medians for the control and Cytochalasin treated fibroblast, respectively. $P<0.05$ was considered statistically significant.

3. RESULTS AND DISCUSSION

3.1. Cell elasticity

Cell elasticity was calculated using only the part of force curve taken during cell loading, assuming in addition that a living cell is an ideally elastic and isotropic material. Figure 2 shows the elasticity results for cardiac fibroblasts, calculated using the AFM force-deformation data up to deformation of 10% since this range has been considered typical of a linear elastic deformation. Median data for the elasticity of control fibroblasts is 1134,2 ± 189,1 Pa, for fibroblasts treated with 0.5 μM Cytochalasin the elasticity is down to 405,4 ± 164,2 Pa. Elasticity data were not normally distributed: in this case, the median better reflects the elasticity of a randomly sampled object, therefore our figures show boxplots which display differences between populations without making any assumptions of the underlying statistical distribution: they are non-parametric. Data shown are those obtained with the lower Cytochalasin concentration (0.5 μM) since this concentration was enough to produce a sensible different behavior in both elasticity and adhesion. Higher Cytochalasin concentration produced test problems since the cell easily detached from the substrate. As shown in Figure 3 (immunofluorescence microscopy and 3D reconstruction of an AFM scan), 0.5 μM of Cytochalasin is enough to disorder the actin filaments. The control cell cytoskeleton looks well spread and almost flat, the cells treated show cytoskeletal morphological changes such as cytoplasmic condensation with formation of phase-dense aggregates.

3.2. Loading/unloading curves

Figure 4 shows the typical AFM force-deformation for control cardiac fibroblasts. The force curve starts with a very short non-linear part of low slope associated with the compression of the thin outside cell membrane that is of gel-like nature. This is followed by a quite extensive linear part. The linear region extends for about 10–15% of cell height deformation. When the tip is brought into contact (the loading phase) with the cell surface receptors, the sphere and receptors bind with attractive forces. Upon sphere retraction, bonds (adhesion) keep them in contact to a certain retract distance. The bond finally breaks and the measured de-adhesion area is equivalent to the de-adhesion work. The retrace phase of the force curve may contain multiple quantized steps (multiple bond-breaking points), each representing specific interactions or unbinding events. These curves represent a basis not only for elasticity assessment of the cell itself, but also for evaluating its overall deformation since these curves contain information about long (between the nucleus and cell membrane via

cytoskeleton)-range interactions. Four distinctive features can be derived from these curves: (i) the maximum force recorded during the loading cycle (ii) the AFM cantilever deformation at the point that the loading cycle is finished but before unloading has started (in this paper called “delta” and labeled A in Fig. 4), which indicates a shift in the force detected at the last point of the loading traces and the initial point of the unloading curve, (iii) the hysteresis area between the loading and unloading cycle (labeled B in Fig. 4), and (iv) the area enclosed by the curve and the zero force axis, which reflects de-adhesion of the AFM sphere from the cell membrane (labeled C in Fig. 4). In this case, the detachment events are manifest as short sudden changes in the cantilever force. Analysis of this latter phase may provide insight into several intrinsic properties in the process of detachment which include: (1) the maximum separation force (in absolute value), and (2) a number of small “steps” in the curve, which could be related to the number of bonds broken between the AFM sphere and membrane integrins.

The control cells and those treated with Cytochalasin D display differences in all interesting features of the loading/unloading curves. The “delta”, the AFM cantilever deformation during the “holding” time after the loading cycle is finished, is quite different. Control cells have always a positive value meaning that during the “holding” period the cantilever rises while, cells with Cytochalasin fail to show a similar resistance with the force remaining constant. The “delta” median for control is 3.65 ± 2.02 nN and - 0.63 ± 0.97 nN for the drug treated cells, respectively. Fig. 5 shows that even if there are few positive values for the drug treated, most of the data are negative (and statistically not different than a null value).

As far as adhesion is concerned, forces acting on the cantilever at detachment are of nanonewton magnitude. These force magnitudes, support the idea that a number of transmembrane proteins bridge the gap between the cell and AFM tip, and act in parallel. Fig. 6 shows the maximum separation force between the AFM tip and the cell membrane for control and fibroblasts treated with Cytochalasin D. Even if there is variability, data show a clear statistical difference due to actin depolymerization. The median value for control is 2.28 ± 1.21 nN and for drug treated is 0.90 ± 0.84 nN respectively.

The different behavior, as a result of the inhibition of actin polymerization due to the Cytochalasin administration, can be seen in Figs. 7 and 8. Fig. 7 shows the typical loadingunloading curves for the administration of 0.5 μM Cytochalasin in which it is possible to value the fact that there is an inversion in the “delta” due to the absence of any resistive “push back” from the treated cells (loading curve is above the unloading, respectively). Fig. 8 compares typical curves for control and cells with aggregation of filamentous actin. It is evident that in the case of control cells a higher force for the same deformation is needed, indicating that these cells are stiffer and stronger. Moreover, the maximum separation force is also higher but above all, the detachment area (grey for control) and the detachment process time are much larger.

In both cases, cantilever displacement always returned to its initial zero position after a series of rupture events however; the curve’s part related to adhesion of control fibroblasts shows clearly many steps due to a sequence of rupture events and two main types of pull-off event: short-length jumps in the curve and longer duration “stretching events”. In control

cells, an initial large peak is always followed by smaller peaks and the whole process continues for a distances of 100–400 nm, presumably arising from the breakage of multiple transmembrane protein: AFM sphere adhesions. However, we were not able to assess a clear correlation between force magnitude and distance from the surface. In the case of cells treated with Cytochalasin, since the cell is softer, the contact area between the AFM sphere and the cell surface might be larger, which should favors the occurrence of multiple interface bonds and increase the total adhesion upon removal. On the contrary, there was a significant decrease in the total number of binding events but not a complete inhibition. The total number of detachments per curve decreases and the adhesion area is much smaller. Moreover, the adhesion events involve a shorter (25–35%) retraction length, indicating that the transmembrane proteins: sphere bond to the controls cells are longer (or can stretch more), in general, than those of Cytochalsin treated cells.

Figure 9 shows the data collected for the detachment area, related to the adhesion phenomenon. We hypothesize that both curves features might be explained taking into consideration the integrins-cytoskeleton interactions and that the different behavior for the Cytochalsin treated cells could be explained if fewer adhesion molecules (such as integrins) are available (or less efficient) for adhesion at the sphere-cell interface. In contrast to the classic continuum models of cell mechanics, in which the applied stress will always quickly dissipate and therefore will not be able to transmit any signals to its surroundings, there are a number of studies, which show that force is directly transmitted from the cytoskeleton to the nucleus and *vice versa*. [37–38]. In this respect, the filaments of the cytoskeleton form the most important part of the mechanical structure in the cell. In particular, actin filaments are connected to the cell membrane through the cell adhesion molecules (mainly integrins), and to the nucleus through the nesprin- and SUN-proteins. Actin resists deformation at low strains and is quickly able to recover initial conformation after long periods of strain, but quickly depolymerizes when it is stretched over 20% of its original dimensions [39]. When cells experience external stress and/or new environments, actin can therefore re-polymerized to handle these changes. Actin filaments are therefore able to effectively transmit forces to the nucleus and *vice versa* from the nucleus to the cell membrane, via integrins and the dystrophin complex [40]. The integrity of such a complex network is of vital importance. All the individual elements form one interacting mechanical entity that cannot function properly if one the elements is interrupted.

For instance, the cell membrane is a heterogeneous assembly, in which there are domains called membrane rafts with distinctive biological properties. It has been shown that establishing and maintaining these rafts is important for cell sustainability [41–44] and several pathologies are associated with changes in rafts morphology [45–47]. Moreover, there is evidence [48] that the actin cytoskeleton connects with rafts and that these interactions are significant in forming and maintaining integrity of the rafts. These domains have specific functions in cell signaling and motility but also adhesion and the interactions of rafts with the actin maintain these functions. There is therefore, a synergistic interaction between membrane rafts and actin and the latter regulates the clustering of membrane raft proteins in a specific manner and at nanoscale level. In general, membrane rafts first recruit

adhesion receptors (like for instance T-cells surface antigen CD2) [49] that initiate signals for actin polymerization. Actin polymerization in turn generates forces inside the cell.

Therefore, alterations in the cytoskeleton (like those created by Cytochalasin administration) suggest that a link must exist between the membrane receptors and the cytoskeletal filaments beneath the cellular surface and inhibition of actin polymerization has effects on the whole cell mechanical behavior as well as adhesion properties.

The adhesion - receptor interaction was already verified in a recent work by Shen et. al, [50]. Using a passive particle tracking techniques on plated fibroblasts, they showed that rheological properties of cells exhibit receptor-dependencies, and further, that the response of cells to actin disruption also depends on the receptors being engaged.

4. CONCLUSIONS

AFM was used to explore the elasticity and adhesion behavior of primary cultures of mouse cardiac fibroblasts. To confirm the hypothesis that a link exists between the membrane receptors and the cytoskeletal filaments causing therefore changing in both elasticity and adhesion behavior, actin-destabilizing Cytochalsin D was administrated to the fibroblasts. From immunofluorescence observation and AFM loading/unloading curves, cytoskeletal reorganization as well as a change in the elasticity and adhesion was indeed observed.

Median data for the elasticity of control fibroblasts is three times higher than that for fibroblasts treated with 0.5 μM Cytochalasin. The AFM force-deformation curves allowed valuing the different mechanical behavior of the two different cells analyzed: (i) the AFM cantilever deformation during the “holding” time after the loading cycle ending: for control cells the cantilever moves up while cells with Cytochalasin fail to actively resist the cantilever, (ii) the maximum force required to deform control cells is higher and as far as adhesion is concerned, (iii) the maximum separation force, detachment area and the detachment process time are much larger for control compared the Cytochalasin treated cells. All these observation shed light on a functional interplay between cytoskeleton and cell membrane receptors confirming that there is a link between the membrane receptors and the actin filaments. This is a significant issue furnishing further evidence on the close connection between cell mechanics and chemical stimuli in regulating cell signaling. Overall this mechanism represents a chemo-mechanical signaling pathway and has an important effect on the whole cell mechanical behavior as well as its adhesion properties.

Acknowledgments

Financial support from “Foreman-Casali” Foundation, Trieste (Italy) to V.M. and L.M.

NIH grants UL1 RR025780 and RO1 HL69071 to L.M.

MISE-ICE-CRUI 16-06-2010 Project 99, and FVG Region LR 26/2005 Art. 23 to O.S.

REFERENCES

1. McKayed KK, Simpson JC. Actin in Action: Imaging Approaches to Study Cytoskeleton Structure and Function. Cells. 2013; 2:715–731. [PubMed: 24709877]

2. Scita G, Confalonieri S, Lappalainen P, Suetsugu S. Irsp53: crossing the road of membrane and actin dynamics in the formation of membrane protrusions. Trends in Cell Biol. 2008; 18:52–60. [PubMed: 18215522]
3. Gov NS, Gopinathan A. Dynamics of membranes driven by actin polymerization. Biophys J. 2006; 90:454–469. [PubMed: 16239328]
4. Veksler A, Gov NS. Phase transitions of the coupled membrane-cytoskeleton modify cellular shape. Biophys J. 2007; 93:3798–3810. [PubMed: 17704150]
5. Hall A. Rho gtpases and the control of cell behavior. Biochem. Soc. Trans. 2005; 33:891–895. [PubMed: 16246005]
6. Jiang G, Huang AH, Cai Y, Tanase M, Sheetz MP. Rigidity sensing at the leading edge through αvβ3 integrins and rptpα. Biophys. J. 2006; 90:1804–1809. [PubMed: 16339875]
7. Martins GG, Kolega J. Endothelial cell protrusion and migration in three-dimensional collagen matrices. Cell Motil. Cytoskeleton. 2006; 63:101–115. [PubMed: 16395720]
8. Giannone G, Sheetz MP. Substrate rigidity and force define form through tyrosine phosphatase and kinase pathways. Trends Cell Biol. 2006; 16:213–223. [PubMed: 16529933]
9. Kabaso D, Shlomovitz R, Schloen K, Stradal T, Gov NS. Theoretical Model for Cellular Shapes Driven by Protrusive and Adhesive Forces. PLoS Comput. Biol. 2011; 7(5):e1001127. [PubMed: 21573201]
10. Hynes RO. Integrins: bidirectional, allosteric signaling machines. Cell. 2002; 110:673–687. [PubMed: 12297042]
11. Legate KR, Wickstroem SA, Faessler R. Genetic and cell biological analysis of integrin outside-in signaling. Genes Dev. 2009; 23:397–418. [PubMed: 19240129]
12. Friedland JC, Lee MH, Boettiger D. Mechanically activated integrin switch controls alpha5beta1 function. Science. 2009; 323:642–644. [PubMed: 19179533]
13. Shen X, Falzon M. Pth-related protein modulates pc-3 prostate cancer cell[50 adhesion and integrin subunit profile. Mol. Cell. Endocrinol. 2003; 199:165–177. [PubMed: 12581888]
14. Van Den Brule F, Califice S, Garnier F, Fernandez PL, Berchuck A, Castronovo V. Galectin-1 accumulation in the ovary carcinoma peritumoral stroma is induced by ovary carcinoma cells and affects both cancer cell proliferation and adhesion to laminin-1 and fibronectin. Lab. Invest. 2003; 83:377–386. [PubMed: 12649338]
15. Mason MD, Davies G, Jiang WG. Cell adhesion molecules and adhesion abnormalities in prostate cancer. Crit. Rev. Oncol. Hematol. 2002; 41:11–28. [PubMed: 11796229]
16. Righi L, Deaglio S, Pecchioni C, Gregorini A, Horenstein AL, Bussolati G, Sapino A, Malavasi F. Role of cd31/platelet endothelial cell adhesion molecule-1 expression in in vitro and in vivo growth and differentiation of human breast cancer cells. Am. J. Pathol. 2003; 162:1163–1174. [PubMed: 12651608]
17. Campbell KP. Three muscular dystrophies: loss of cytoskeleton extracellular matrix linkage. Cell. 1995; 80:675–679. [PubMed: 7889563]
18. Angoli D, Corona P, Baresi R, Mora M, Wanke E. Lamininalpha2 but not -alpha1-mediated adhesion of human (duchenne) and murine (mdx) dystrophic myotubes is seriously defective. FEBS Lett. 1997; 408:341–344. [PubMed: 9188790]
19. Lal R, John SA. Biological applications of atomic force microscopy. Am. J. Physiol. 1994; 266:C1–C21. [PubMed: 8304408]
20. Kuznetsova TG, Starodubtseva MN, Yegorenkov NI, Chizhik SA, Zhdanov RI. Atomic force microscopy probing of cell elasticity. Micron. 2007; 38:824–833. [PubMed: 17709250]
21. Reif M, Gautel M, Oesterhelt F, Fernandez JM, Gaub HE. Reversible unfolding of individual titin immunoglobulin domains by AFM. Science. 1997; 276:1109–1112. [PubMed: 9148804]
22. Yuan C, Chen A, Kolb P, Moy VT. Energy landscape of the streptavidin-biotin complexes measured by atomic force microscopy. Biochemistry. 2000; 39:10219–10223. [PubMed: 10956011]
23. van den Borne SWM, Diez J, Blankesteijn WM, Verjans J, Hofstra L, Narula J. Myocardial remodeling after infarction: the role of myofibroblasts. Nat. Rev. Cardiol. 2009; 7:30–37. [PubMed: 19949426]

24. Parker KK, Ingber DE. Extracellular matrix, mechanotransduction and structural hierarchies in heart tissue engineering. Philos. Trans. R. Soc. London B Biol. Sci. 2007; 362:1267–1279. [PubMed: 17588874]
25. Towbin JA, Bowles KR, Bowles NE. Etiologies of cardiomyopathy and heart failure. Nature Med. 1999; 5:266–267. [PubMed: 10086375]
26. Towbin JA. The role of cytoskeletal proteins in cardiomyopathies. Curr. Opin. Cell Biol. 1998; 10:131–139. [PubMed: 9484605]
27. Rotsch C, Radmacher M. Drug-Induced Changes of Cytoskeletal Structure and Mechanics in Fibroblasts: An Atomic Force Microscopy Study. Biophys. J. 2000; 78:520–535. [PubMed: 10620315]
28. Sirghi L, Ponti J, Broggi F, Rossi F. Probing elasticity and adhesion of live cells by atomic force microscopy indentation. Europ. Biophysics J. 2008; 37:935–945.
29. Reif M, Gautel M, Oesterhelt F, Fernandez JM, Gaub HE. Reversible unfolding of individual titin immunoglobulin domains by AFM. Science. 1997; 276:1109–1112. [PubMed: 9148804]
30. Yuan C, Chen A, Kolb P, Moy VT. Energy landscape of the streptavidin-biotin complexes measured by atomic force microscopy. Biochemistry. 2000; 39:10219–10223. [PubMed: 10956011]
31. Weisenhorn AL, Khorsandi M, Kasas S, Gotzos V, Butt HJ. Deformation and height anomaly of soft surfaces studied with an AFM. Nanotechnology. 1993; 4:106–113.
32. Radmacher M, Fritz M, Hansma PK. Imaging soft samples with the atomic force microscope: gelatin in water and propanol. Biophys. J. 1995; 69:264–270. [PubMed: 7669903]
33. Johnson KL, Kendall K, Roberts AD. Surface energy and the contact of elastic solids. Proc. R. Soc. Lond. Ser. A. 1971; 324:301–321.
34. Ohashi T, Ishii Y, Ishikawa Y, Matsumoto T, Sato M. Experimental and numerical analyses of local mechanical properties measured by atomic force microscopy for sheared endothelial cell. BioMed. Mater. Eng. 2002; 12:319–327. [PubMed: 12446947]
35. Kuznetsova GT, Starodubtseva MN, Yegorenkov NI, Chizhik SA, Zhdanov RI. Atomic force microscopy probing of cell elasticity. Micron. 2007; 38:824–833. [PubMed: 17709250]
36. Rico, F.; Wojcikiewicz, EP.; Moy, VT. Atomic force microscopy studies of the mechanical properties of living cells. In: Bharat, Bhushan; Harald, Fuchs; Masahiko, Tomitori, editors. Appl. Scanning Probe Methods IX, NanoScience and Technology. N. Y.: Springer-Verlag; 2008. p. 89-109.
37. Guilak F. Compression-induced changes in the shape and volume of the chondrocyte nucleus. J Biomech. 1995; 28:1529–1541. [PubMed: 8666592]
38. Maniotis AJ, Chen CS, Ingber DE. Demonstration of mechanical connections between integrins, cytoskeletal filaments, and nucleoplasm that stabilize nuclear structure. Proc. Natl. Acad. Sci. U S A. 1997; 94:849–854. [PubMed: 9023345]
39. Janmey PA, Euteneuer U, Traub P, Schliwa M. Viscoelastic properties of vimentin compared with other filamentous biopolymer networks. J. Cell Biol. 1991; 113(1):155–160. [PubMed: 2007620]
40. Cattin ME, Bertrand AT, Schlossarek S, Le Bihan MC, Skov JS, Neuber C, Crocini C, Maron S, Lainé J, Mougenot N, Varnous S, Fromes Y, Hansen A, Eschenhagen T, Decostre V, Carrier L, Bonne G. Heterozygous LmnadelK32 mice develop dilated cardiomyopathy through a combined pathomechanism of haplo insufficiency and peptide toxicity. Hum. Mol. Genet. 2013; 22(15): 3152–3164. [PubMed: 23575224]
41. Yang B, Oo TN, Rizzo V. Lipid rafts mediate H_2O_2 prosurvival effects in cultured endothelial cells. FASEB J. 2006; 20:1501–1503. [PubMed: 16754746]
42. Yamazaki S, Iwama A, Takayanagi S, Morita Y, Eto K, Ema H, Nakauchi H. Cytokine signals modulated via lipid rafts mimic niche signals and induce hibernation in hematopoietic stem cells. EMBO J. 2006; 25:3515–3523. [PubMed: 16858398]
43. Furne C, Corset V, Herincs Z, Cahuzac N, Hueber AO, Mehlen P. The dependence receptor DCC requires lipid raft localization for cell death signaling. Proc. Natl. Acad. Sci. USA. 2006; 103:4128–4133. [PubMed: 16537496]

44. Koenig A, Russell JQ, Rodgers WA, Budd RC. Spatial differences in active caspase-8 defines its rolein T cell activation versus cell death. Cell Death Differ. 2008; 15:1701–1711. [PubMed: 18617900]
45. Baruthio F, Quadroni M, Ruegg C, Mariotti A. Proteomic analysis of membrane rafts of melanoma cells identifies protein patterns characteristic of the tumor progression stage. Proteomics. 2008; 8:4733–4747. [PubMed: 18942674]
46. Jury EC, Kabouridis PS, Flores-Borja F, Mageed RA, Isenberg DA. Altered lipid raft-associated signaling and ganglioside expression in T lymphocytes from patients with systemic lupus erythematosus. J. Clin. Invest. 2004; 13:1176–1187. [PubMed: 15085197]
47. Banfi C, Brioschi M, Wait R, Begum S, Gianazza E, Fratto P, Polvani G, Vitali E, Parolari A, Mussoni L, Tremoli E. Proteomic analysis of membrane microdomains derived from both failing and nonfailing human hearts. Proteomics. 2006; 6:1976–1988. [PubMed: 16475230]
48. Liu AP, Fletcher DA. Actin polymerization serves as a membrane domain switch in model lipid bilayers. Biophys. J. 2006; 91:4064–4070. [PubMed: 16963509]
49. Yang H, Reinherz EL. Dynamic recruitment of human CD2 into lipid rafts. Linkage to T cell signal transduction. J. Biol. Chem. 2001; 276:18775–18785. [PubMed: 11376005]
50. Shen MY, Michaelson J, Huang H. Rheological responses of cardiac fibroblasts to mechanical stretch. Biochem. Biophys. Res. Comm. 2013; 430:1028–1033. [PubMed: 23261449]

Highlights

- The whole AFM force-deformation cell curves were analyzed
- They provide information on both the elasticity and adhesion behavior
- Actin-destabilizing Cytochalsin D was administrated to the fibroblasts
- Change in elasticity and adhesion was ascribed to cytoskeletal reorganization
- A link exists between the membrane receptors and the cytoskeletal filaments

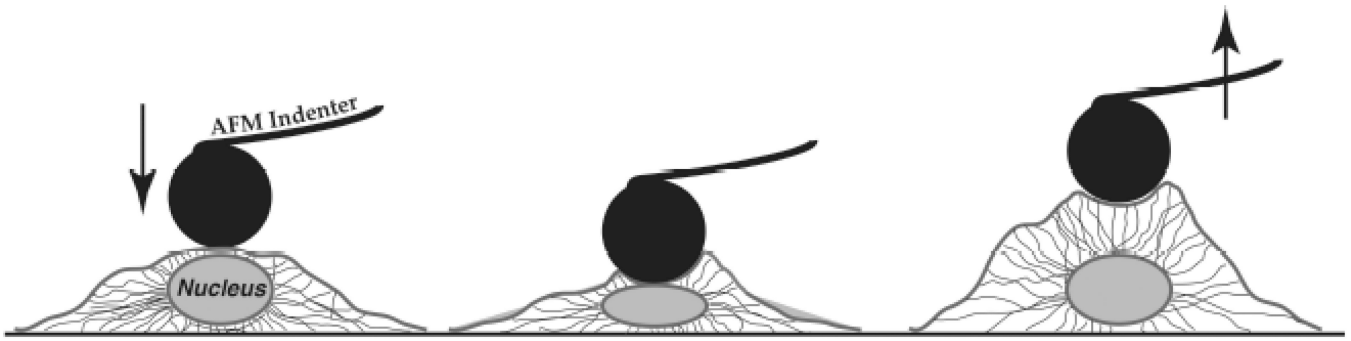

Fig. 1.

Schematic of the AFM force experiment representing a spherical AFM probe used to apply (1) a constant downward mechanical force to the nucleus of a cell, (2) a holding time, (3) an unloading at constant speed.

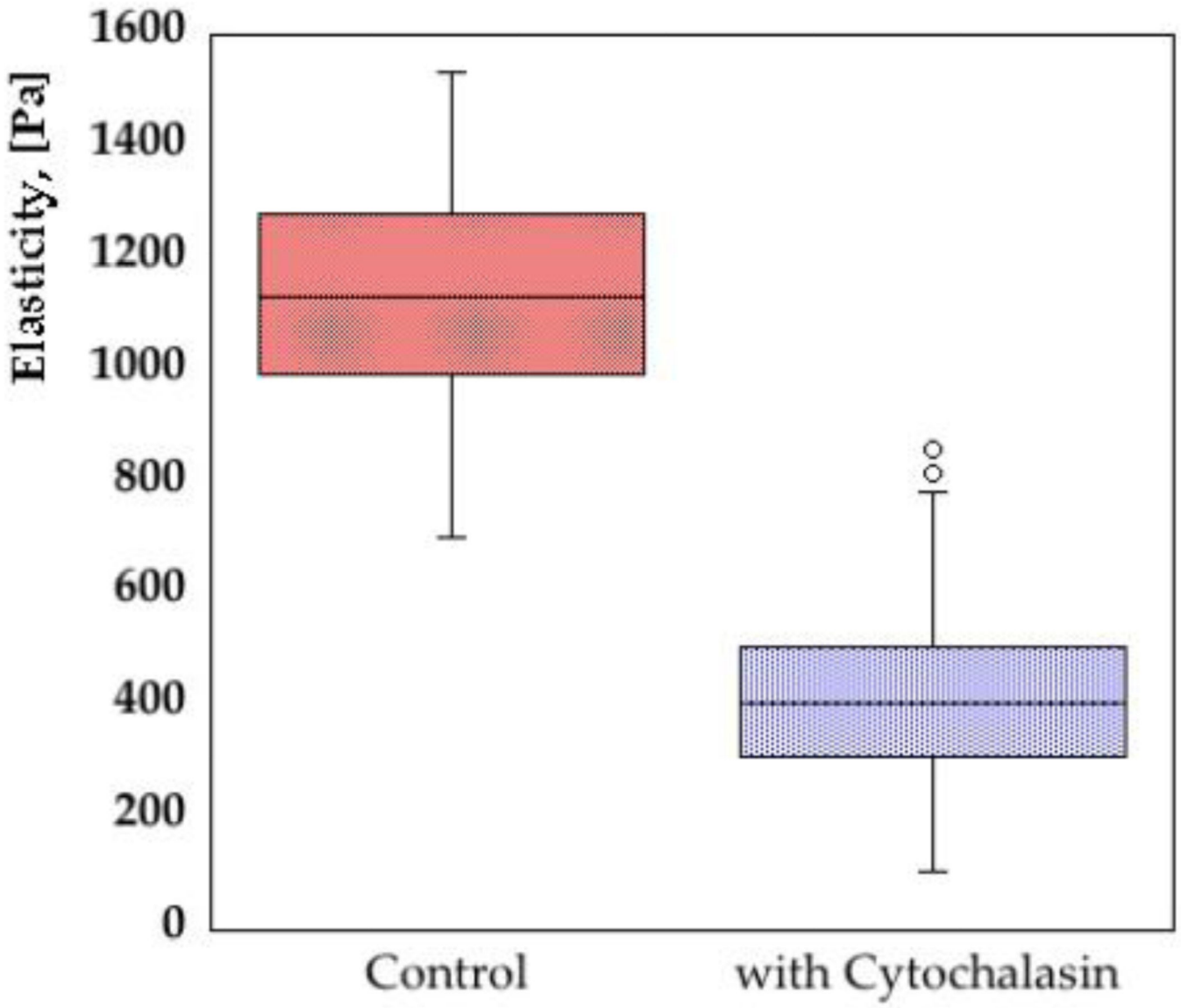

Fig. 2.

Elasticity (Young Modulus) for cardiac fibroblast with and without Cytochalasin. Data are presented as a box whose endpoints are the first quartile: and third quartile, with a horizontal line corresponding to the second quartile (median). The spacing between the different parts of the box indicates the degree of dispersion (spread) and skewness in the data, and identifies outliers. Data marked with dots are called outliers.

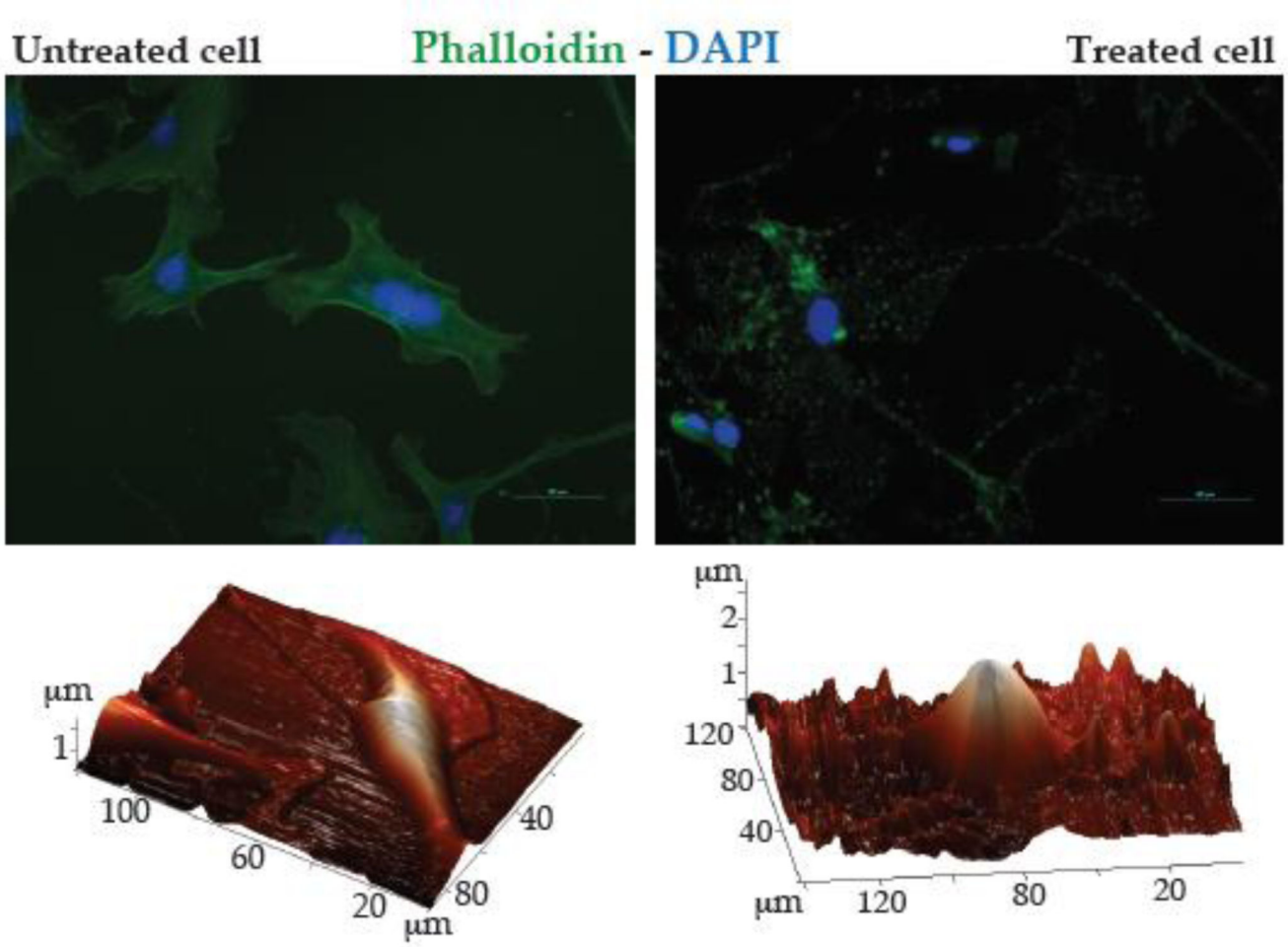

Fig. 3.

Effect of Cytochalasin D on cell shape. Top: Immunofluorescence microscopy of cardiac fibroblasts in control, untreated cells (left) or after Cytochalasin D treatment (right). Cytochalasin D-treatment cells resulted in consistent changes in the cytoskeleton configuration and density, with a dramatic disruption of the actin network. Cardiac fibroblasts were stained for green antibody. Nuclei were counterstained with DAPI (blu). Bar: 50 µm. Bottom: AFM 3D reconstruction of control cardiac fibroblasts morphology (left), after Cytochalasin administration (right).

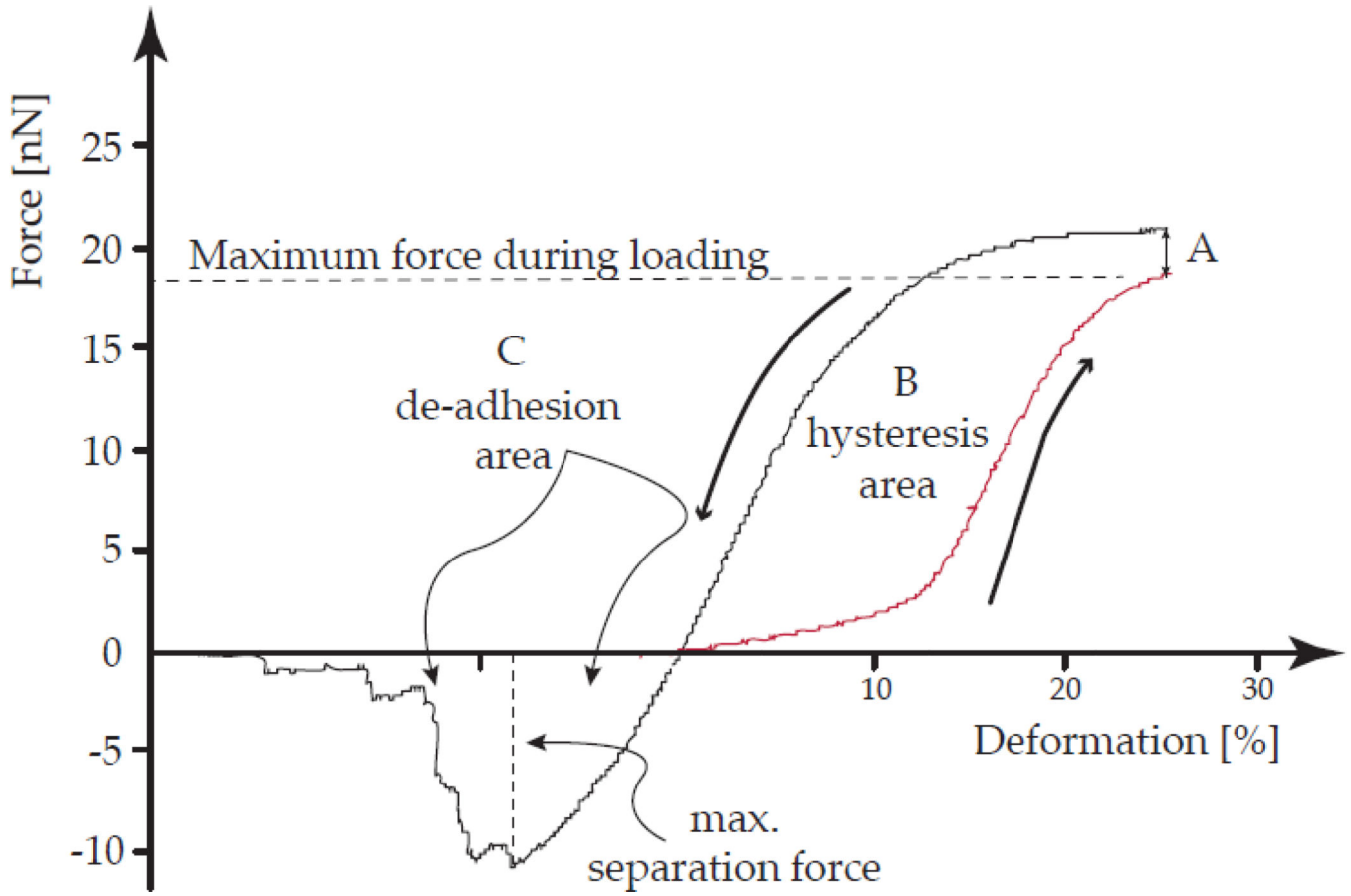

Fig. 4.

Typical loading-unloading AFM curve for a control fibroblasts. In red the loading in black the unloading cycle, respectively

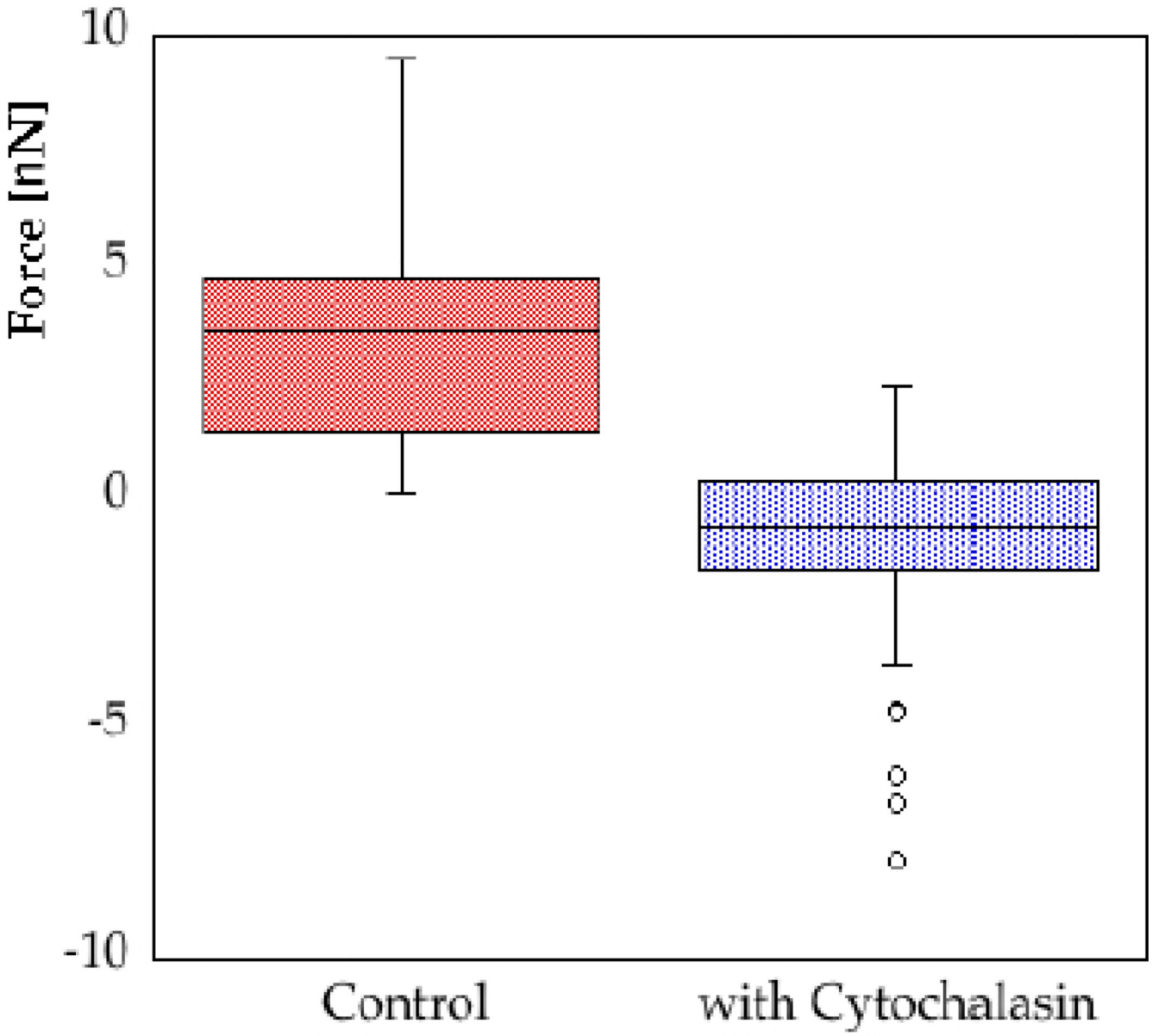

Fig. 5.

The “delta” a shift in the force detected at the last point of the loading traces and the initial point of the unloading curve for control and fibroblasts treated with Cytochalasin D, respectively ($p<0.0001$)

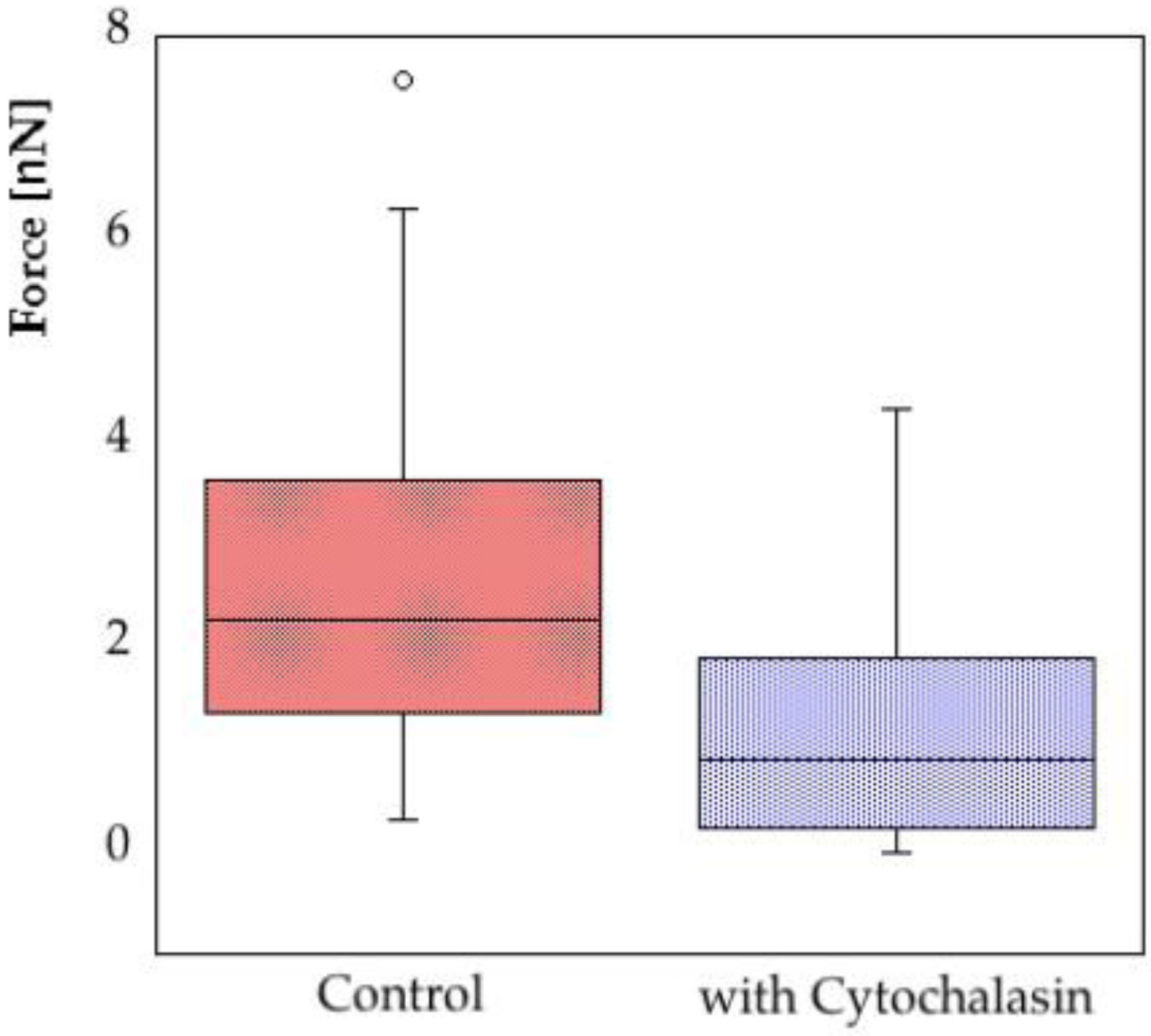

Fig. 6.

Maximum separation force for control and fibroblasts treated with Cytochalasin D, respectively ($p<0.0001$)

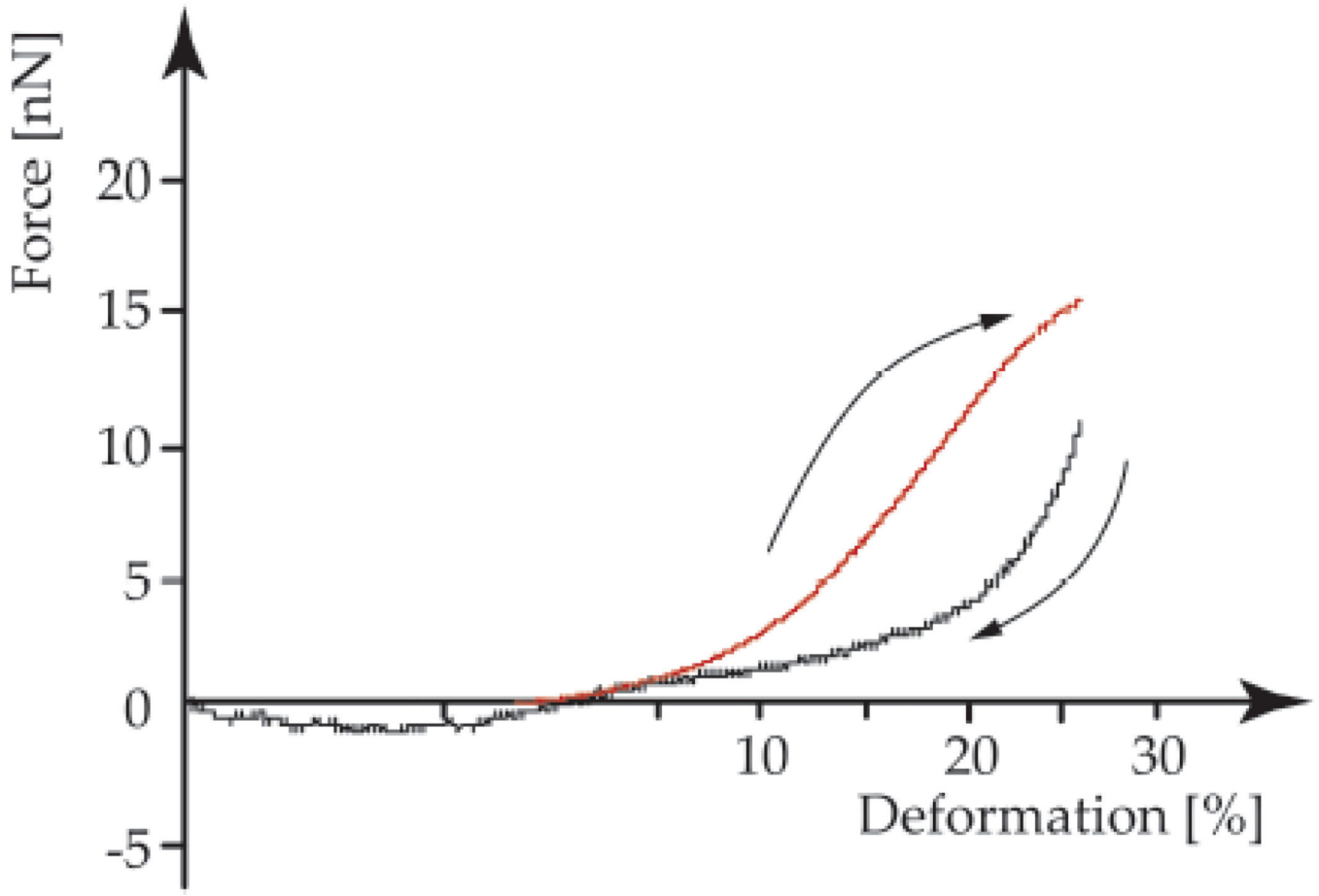

Fig. 7.
Loading-unloading curves for fibroblast after Cytochalasin administration

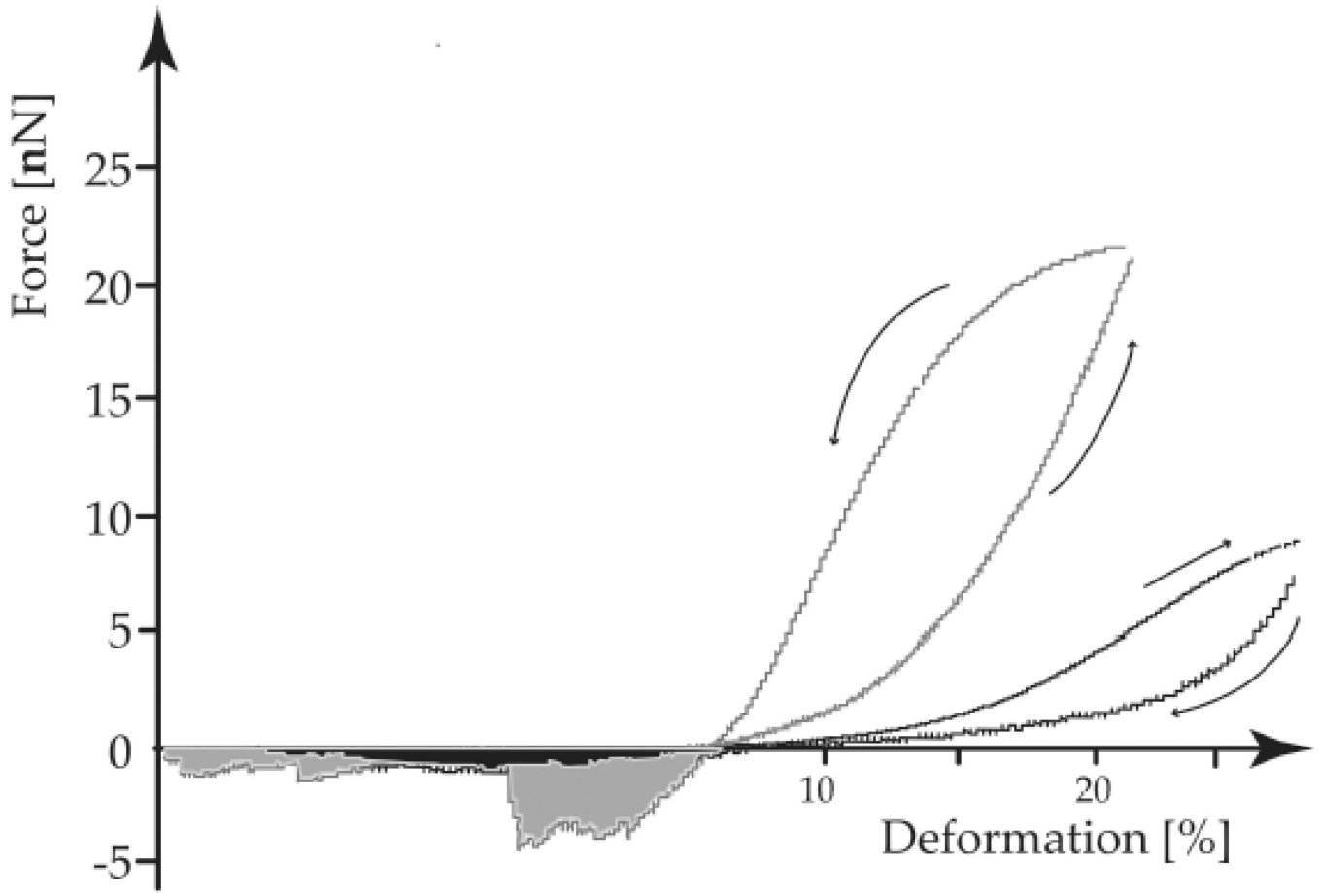

Fig. 8.

Loading-unloading curves for control and Cytochalasin fibroblast after Cytochalasin administration. In grey the adhesion area for control and in black Cytochalasin added drug, respectively

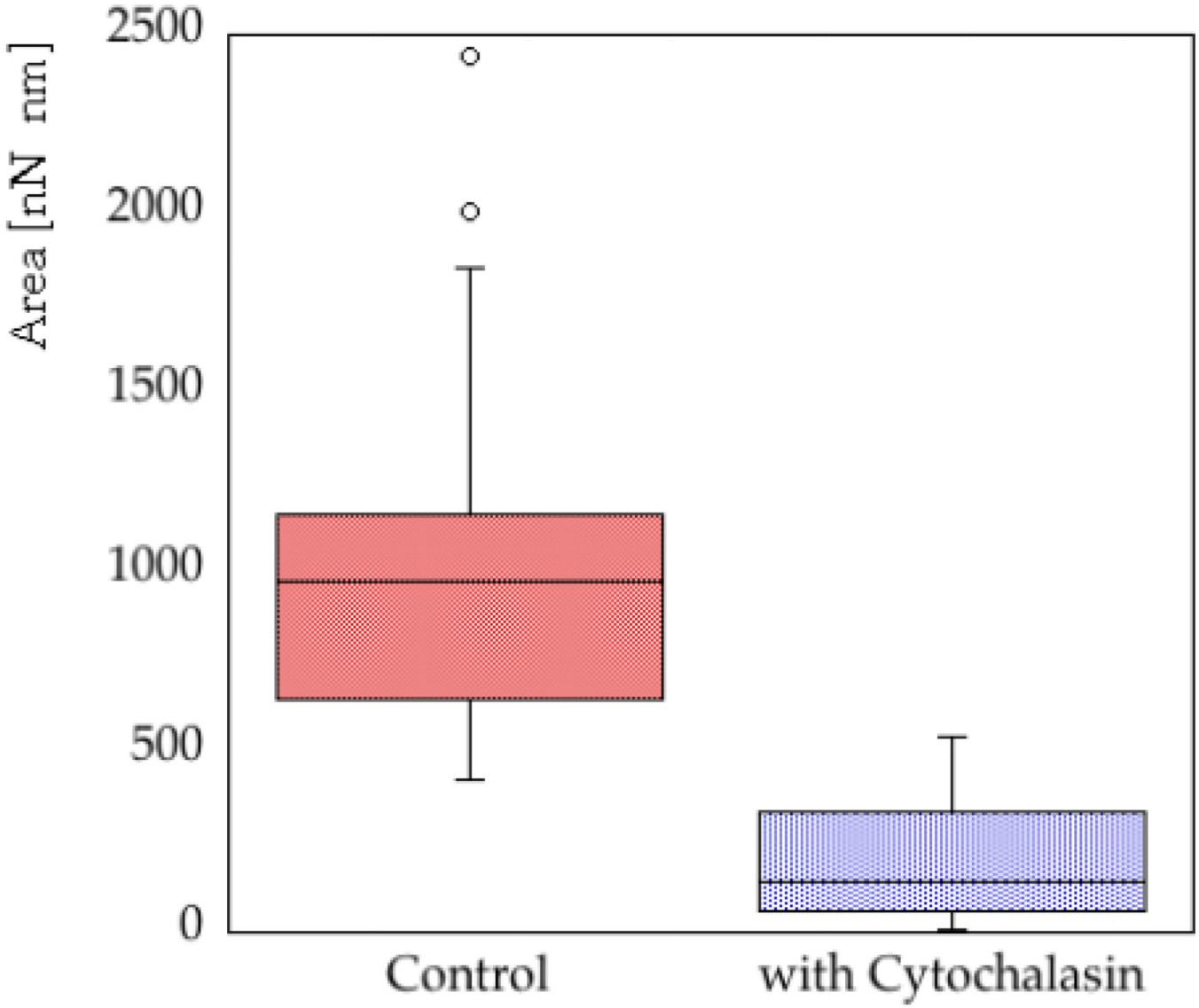

Fig. 9.

Boxplot for the detachment area enclosed by the AFM unloading curve and the zero force axis. For control cells median is 976±87.9 (nN nm) for Cytochalasin treated is 139± 28.3 (nN nm) ($p<0.0001$), respectively.